Available online at www.sciencedirect.com
SCIENCE DIRECT®
Biochimica et Biophysica Acta 1612 (2003) 144–153
BIOCHIMICA ET BIOPHYSICA ACTA
BBA
www.bba-direct.com

Probing the volume changes during voltage gating of Porin 31BM channel with nonelectrolyte polymers

Carlos M.M. Carneiro[a], Petr G. Merzlyak[a], Liliya N. Yuldasheva[a], Leandro G. Silva[a], Friedrich P. Thinnes[b], Oleg V. Krasilnikov[a,*]

[a] *Laboratory of Membrane Biophysics, Department of Biophysics and Radiobiology, Federal University of Pernambuco, 50670-901, Recife, PE, Brazil*
[b] *Max-Plank Institute of Experimental Medicine, Göttingen, Germany*

Received 4 September 2002; received in revised form 13 February 2003; accepted 4 April 2003

Abstract

To probe the volume changes of the voltage-dependent anion-selective channel (VDAC), the nonelectrolyte exclusion technique was taken because it is one of the few existing methods that may define quite accurately the rough geometry of lumen of ion channels (in membranes) for which there is no structural data.

Here, we corroborate the data from our previous study [FEBS Lett. 416 (1997) 187] that the gross structural features of VDAC in its highest conductance state are asymmetric with respect to the plane of the membrane, and state that this asymmetry is not dependent on sign of voltage applied. Hence, the plasticity of VDAC does not play a role in the determination of lumen geometry at this state and the asymmetry is an internal property of the channel.

We also show that the apparent diameter of the cis segment of the pore decreases slightly from 2 to 1.8 nm when the channel's conductance decreases from its high to low state. However, the trans funnel segment undergoes a more marked change in polymer accessible volume. Specifically, its larger diameter decreases from ~ 4 to 2.4 nm. Supposing the channel's total length is 4.6 nm, the apparent change in channel volume during this transition is estimated to be about 10 nm^3, i.e. about 40% of the channel's volume in the high conductance state.

Keywords: Ion channel; Lipid bilayer; VDAC; Volume change

1. Introduction

Protein pores (ion channels) possess several properties such as conductance, selectivity and gating. There are growing indications that the electrical properties of single ion channels, called ''gating'', are correlated with its structural modifications. All geometric models developed to describe this behavior can be roughly divided into two classes: ''blocking'' and ''rearrangement''. It appears that voltage-dependent K^+ channels are a striking example of the first model of gating [1], while voltage-dependent anion-selective channel (VDAC) [2,3] and gap junction [4] are representatives of the second model of gating. Measurement of the changes in the internal channel volume is very helpful in distinguishing between these two classes of models. However, there are few methods available for channels for which there is no structural data [2,5]. Given the interest in this area, it is of fundamental importance to develop new methods to measure changes in internal channel volume with channel opening and closing. Here we introduce an approach that bases on nonelectrolyte exclusion method, developed recently to define the internal geometry of pores [6]. Bovine muscle porin (Porin-31BM channel) was used in our investigation. Based on the channel geometry in high and low conductance states, the apparent change in the channel volume during this transition is estimated to be of ~ 10 nm^3. The

* Corresponding author. Depto. de Biofisica e Radiobiologia, Centro de Ciencias Biologicas, Universidade Federal de Pernambuco, Cidade Universitaria, Av. prof. Moraes Rego, S/N, Recife, Pernambuco, CEP 50670-901, Brazil. Tel.: +55-81-327-18535; fax: 55-81-327-18560.
E-mail address: kras@ufpe.br (O.V. Krasilnikov).

0005-2736/03/$ - see front matter © 2003 Elsevier Science B.V. All rights reserved.
doi:10.1016/S0005-2736(03)00113-5

procedure should be applicable to other ion channels and to related structures.

2. Materials and methods

2.1. Materials

VDAC was isolated from bovine muscle by using methods described elsewhere [7] for VDAC from human tissue. Pure phosphatidylcholine and cholesterol were purchased from Sigma Chemical Co., St. Louis, MO. Polyethylene glycols, such as PEG300 and PEG400 (Sigma), PEG600 (Riedel de Haën, Quimibrás Industrias Quimicas, S.A., Brazil), PEG1000 and PEG1450 (Sigma), PEG2000, PEG3000 and PEG4000 (Loba Chemie, Mumbai, India), PEG8000 and PEG12000 (Sigma) were used. The hydrodynamic radii of PEGs determined by viscometry were taken from [8]. The authors used a glass capillary viscometer with low stream of solution to avoid the deformation of the polymer shape by the shear forces and found the following values to hydrodynamic radii: 0.60 ± 0.03 nm PEG300; 0.70 ± 0.03 nm PEG400; 0.80 ± 0.04 nm PEG600; 0.94 ± 0.03 nm PEG1000; 1.05 ± 0.03 nm PEG1450; 1.22 ± 0.03 nm PEG2000; 1.44 ± 0.03 nm PEG3000; 1.92 ± 0.03 nm PEG4000; 2.1 ± 0.03 nm PEG4600. The number average (M_n) and weight average (M_w) molecular masses of the polymers were determined by gel permeation chromatography. The ratio M_w/M_n indicates the mass distribution of a polymer and it was found to increase with molecular mass of a polymer from 1.08 (for PEG400) to 1.18 (for PEG4600). This is indicative of moderate dispersibility of PEGs that, notwithstanding, does not apparently hamper channel sizing experiments [9]. Other chemicals were of analytical grade.

3. Methods

3.1. General aspects

Double distilled water was used to prepare all aqueous solutions. Unless stated otherwise, standard solution used in the bilayer experiments contained 1.15 M KCl and 5 mM HEPES and the pH was adjusted to 7.0 with 1.0 M KOH. In channel sizing experiments, this solution also contained 20% (w/v) of an appropriate molecular weight PEG. Black lipid membranes (BLM) were formed at room temperature 25 ± 2 °C by the Mueller method [10] from a phosphatidylcholine–cholesterol mixture (3:1, mass/mass). Bilayer experiments were performed under voltage-clamp conditions in essentially the same manner that has been described recently [11]. Bilayers were not rebuilt when VDAC was already present in the bathing solution.

The amplifier signal was monitored with a storage oscilloscope (Model 201, Nicolet Technologies, Madison, WI) as well as with the IBM-compatible 486/487 100 MHz computer with DT01-EZ 12 bit A/D converter board (Data Translation). Whole Cell Electrophysiology Program (WCP V1.7b, J. Dempster) software was used. Upward current steps (Fig. 1A) were measured and single channel conductances were estimated by dividing the single channel current by the voltage imposed through the membrane. Cumulative histograms of the events at all experimental conditions were made. The histograms were not uniform. A sum of two to three theoretical normal distributions was needed to fit its. Microcal Origin software was utilized for this aim. Mean value of the main pool of the channel events was used for subsequent analysis.

In most experiments, positive (10 or 50 mV) voltage pulses were applied to the cis compartment of the chamber,

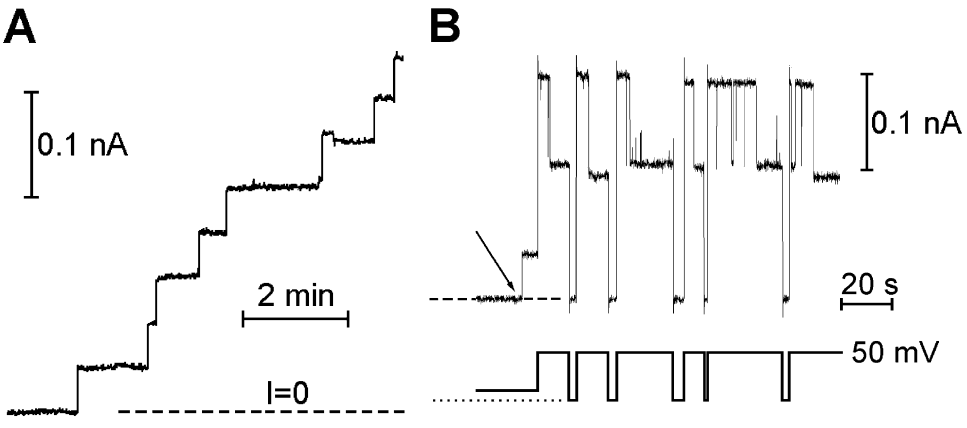

Fig. 1. Original recordings of VDAC insertion (A) and the transitions of the single channel to the low conductance state (B). The dashed lines indicate the zero current level. The dotted line indicates the zero voltage level. Current and time scales are given in the figure. Solution contains 1.15 M KCl, 5 mM HEPES, pH 7. VDAC was added in the cis compartment. In experiments with VDAC insertion (A) potential was +10 mV. For the channel closing experiments (B) the voltage protocol is shown in the figure. The arrow indicates the moment of the channel insertion at +10 mV. Then the potential was switched to 50 mV. This forced the channel to go to a low conductance state. In order to reopen the channel, the potential was transiently switched to 0 mV and the back to 50 mV again.

which was defined as the side of Porin 31BM addition. The polarity was chosen to simulate the conditions in the outer mitochondrial membrane, where a positive value of potential is expected on the side of protein insertion, because VDAC is synthesized in the cytoplasm and only then incorporated into the outer mitochondrial membrane [12]. In a separate set of experiments the negative voltage pulses were used to verify whether the direction of the electric field affects the lumen geometry of VDAC channel in its high conductance state. In our previous work [11] and this study VDAC channels appeared to have a similar orientation in membranes because the established asymmetry in the lumen geometry is only possible if VDAC channels are invariably oriented. Our observations are in accordance with data obtained with channels formed by other mammalian porin, e.g. Porin 31HL, in lipid bilayers [13] where the authors had noted that in response to positive and negative voltage pulses "the current decreased in a somewhat asymmetric fashion which suggested asymmetric insertion of the channels into the membrane".

These and several other publications contradict the widely accepted point of view that VDAC inserts into planar lipid bilayers in random orientation. The reason of this discrepancy is not clear now and is not a topic of this study.

3.2. Sizing of VDAC

To find changes in internal channel volume with channel opening and closing, one needs to know the parameters of the channel lumen at these two states. Geometric parameters of the Porin 31BM channel in high conductance state were taken from our previous study [11], which was additionally improved (as regards to access resistors correction) and completed with new results obtained with opposite (negative) sign of voltage pulses (− 10 mV) on the side of protein addition.

To analyze the channel lumen geometry in low conductance state, the bilayer was initially clamped at 10 mV. When a channel appeared, its conductance was measured and the potential was changed to 50 mV. This caused VDAC to switch to its low conductance state. To reopen the channel to its high conductance state, the transmembrane potential was transiently set to 0 mV and then back again to 50 mV (Fig. 1B). Experiments with different PEGs placed in contact with one of the openings of the channel were done. The low conductance values for each individual channel were determined, and the results obtained for different channels under the same conditions were summarized in the cumulative histogram and analyzed in the same manner, as was done for the case of VDAC in high conductance state.

Because several theoretical issues concerning polymer partitioning into a channel pore are still unresolved even in the case of symmetric polymer addition, we used here an empirical approach to analyze polymer partitioning under asymmetrical conditions. We assumed that if the PEG hydrodynamic radius is smaller than the opening of the channel, PEG partitions freely into the pore and occupies (with a concentration proportional to its bulk concentration) all the space available before the narrowest constriction prevents the polymer from partitioning further into the pore. If the PEG hydrodynamic radius is larger than the pore's radius at the opening, it cannot partition into the pore. Thus, if PEGs enter the channel lumen of a given channel, the conductance of that channel decreases. On the other hand, molecules that do not enter the lumen should not significantly alter single channel conductance.

In the asymmetric addition of polymer system used here, the bulk conductivity of the solutions and the activity of ions on both sides of the membrane were identical. The slight difference in osmolalities should not generate a strong water flow through the channel or a detectable transmembrane potential [14].

The mean values of the main pool of single channel conductances and bulk conductivities are used to establish the filling (F) of the channel with PEG through one of it openings (see below). The geometrical features of the VDAC lumen were established using a two-step procedure. First, the VDAC single channel conductance data were used to calculate the filling of the channel with PEG as described elsewhere [15] and the sizes of the cis and the trans openings were estimated from the dependence of F on the hydrodynamic radius of the polymer.

Second, the single channel conductance data were corrected for the access conductance (g^{acc}), which was calculated in accordance with Hall [16] for each opening:

$$g^{acc} = 4r\chi$$

where r is the radius for the channel opening and χ is the solution conductivity.

The corrected conductance data were used throughout this study to calculate the channel filling F with PEG using following equation:

$$F = \left(\frac{g_0 - g_i}{g_i}\right) \Big/ \left(\frac{\chi_0 - \chi_i}{\chi_i}\right)$$

where g_0 is the single channel conductance in the polymer-free solution; g_i is the single channel conductance in the presence of PEG with access to the channel interior on one side only (g_i^{cis} or g_i^{trans}) while PEG4600 was on the other side; χ_0 and χ_i are the conductivities of the polymer-free solution and the solution containing 20% (w/v) of a given polymer, respectively.

The filling parameter, F, is plotted against the hydrodynamic radius of PEG, and the geometry of VDAC lumen was finally deduced from this dependence. Small PEGs penetrate the VDAC channel. Increasing the size of the PEG produces a decrease in F until a constant lower limit is attained. The intercept between the linear inverse relation and the invariant lowest portion of the parameter F on the hydrodynamic radius of PEG was assumed to be the

maximum radius of the channel opening. In addition, a change in the slope of the inverse linear relation between F and PEG hydrodynamic radius was assumed to reflect a change in geometry of the channel along its lumen. This method provides an estimate for the maximum size of both channel openings with ± 0.1 nm accuracy. The length of the channel segments with different geometries can be determined with less precision.

The polymer-exclusion method assumes the absence of interaction between PEG and a channel wall (but see Refs. [9,17,18]) and gives the correct values for channel geometry only if this assumption is true [6,9]. Although we used a relatively high concentration of the electrolyte, F was smaller than 1 for VDAC channel in high conductance state at symmetric (data not shown) and asymmetric nonelectrolyte addition. F for VDAC in low conductance state was over 1, but the excess was not large. This suggests the absence of sizeable nonspecific hydrophobic interactions between PEG and the channel lumen wall under the conditions used in this study.

4. Results

4.1. Testing of hypothesis of VDAC plasticity in high conductance state

As has been demonstrated recently [11], Porin 31BM channel in high conductance state looks like an asymmetrical channel. If we assume that the channel's total length is 4.6 nm, the cis side of the pore (the side to which VDAC is added) appears roughly as a $\sim$ 2.5-nm-long cylinder with a diameter of $\sim$ 2.0 nm. In contrast, the trans side of the pore has a funnel-like shape that seems $\sim$ 4 nm in diameter at the pore's opening and that tapers to $\sim$ 2 nm in diameter further inside the lumen. This information was drawn from the analysis of $F-r$ dependence with ion channel conductance established at +10 mV. Large portions of the VDAC protein (localized in different parts of the molecule) move through the membrane during the gating [19]. The potential (+10 mV) was far below of that evoked for the VDAC channel gates (>30 mV). However, it is not unreasonable to hypothesize that a small potential utilized to monitoring the VDAC channel in the high conductance state produces some change in the channel geometry in this state also. Thus, it is conceivable that the observed deviation in the VDAC channel geometry from a right circular cylinder can be caused solely by a distortion induced by the applied electric field and the possible plasticity of the VDAC channel.

If such distortion really exists, the geometry of the ion channel lumen with respect to the center of the membrane seen at the positive potential (where the trans opening of the channel is larger than the cis one) should change into its mirror image (with the cis opening larger than the trans one) when the opposite (negative) sign of the potential is applied. We have made such experiments and found that the observed changes in the channel conductances (Table 1) and corresponding filling parameter values (Fig. 2) at the negative and at the positive applied voltage are virtually identical. This suggests that VDAC is not measurably plastic in its high conductance state under the small electric field applied. We further conclude that the established asymmetry in the channel's structure is a property of VDAC in its high conductance state. Moreover, both studies evidently demonstrate that Porin-31BM channels are topologically oriented similarly in planar lipid membranes, since the established stable asymmetry in geometry is only possible if VDAC channels are invariably oriented.

4.2. Role of access conductance

The access conductance can affect significantly the experimental value of channel conductance if the access conductance is in the same order of magnitude as that of the single channel conductance. It is exactly the case of VDAC. The influence of the access conductance in determining the size of an ion channel opening by the polymer-exclusion

Table 1
The access resistance corrected conductances of 31BM-porin channel at the high conductance state as changed by PEG addition

		r, nm	χ, mS/cm	$g\#^{trans}$ (N), +10 mV	$g\#^{trans}$ (N), −10 mV	$g\#^{cis}$ (N), +10 mV	$g\#^{cis}$ (N), −10 mV
1	Control		132.0	5.37 ± 0.2 (212)	5.37 ± 0.2 (212)	5.37 ± 0.2 (212)	5.37 ± 0.2 (212)
2	PEG300	0.6	65.4	2.84 ± 0.4 (140)	–	2.84 ± 0.2 (170)	–
3	PEG400	0.7	62.9	2.88 ± 0.4 (138)	–	2.99 ± 0.2 (178)	–
4	PEG600	0.8	65.2	3.15 ± 0.2 (110)	3.18 ± 0.4 (124)	3.17 ± 0.4 (208)	3.07 ± 0.7 (108)
5	PEG1000	0.94	61.4	3.64 ± 0.4 (155)	3.73 ± 0.5 (160)	5.28 ± 0.5 (193)	5.53 ± 0.3 (112)
6	PEG1450	1.05	63.4	4.22 ± 0.4 (121)	4.62 ± 0.6 (45)	5.25 ± 0.5 (163)	5.15 ± 0.4 (63)
7	PEG2000	1.22	63.3	4.34 ± 0.3 (118)	4.46 ± 0.3 (71)	5.42 ± 0.4 (91)	5.20 ± 0.4 (75)
8	PEG3000	1.44	66.2	4.57 ± 0.3 (116)	–	5.40 ± 0.3 (43)	–
9	PEG4000	1.92	62.2	5.35 ± 0.5 (72)	–	5.35 ± 0.5 (41)	–

χ is the solution conductivity; r is hydrodynamic radii of non-electrolytes. Single-channel conductances with access resistor correction (nS) of the main pool of the events are expressed as mean ± S.D. N is the number of the single channel events. $g\#^{cis}$ was measured in the presence of a given non-electrolyte on the *cis*-side of the bilayer while PEG4600 was present on the *trans*-side and $g\#^{trans}$ refers to the conductance measured in the presence of a given non-electrolyte on the *trans*-side of the bilayer while PEG4600 was present at the *cis*-side. The data presented in columns +10 mV obtained from the rough data of Carneiro et al. [11] by the access resistor correction.

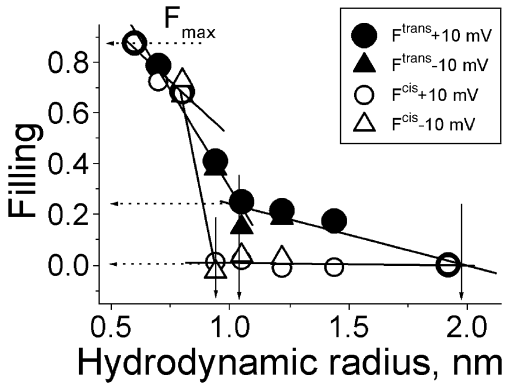

Fig. 2. The dependence of F^{cis} and F^{trans} (obtained for VDAC-channels in fully open state) on the hydrodynamic radii of PEGs. Bovine muscle Porin was always added to the cis compartment to a final concentration of ~4 ng/ml. For cis filling experiments test-PEGs (20% w/v) were added at the cis-opening of the channel, while impermeant PEG4600 (20% w/v) was added to the trans side. For trans filling experiments, test-PEGs were added to the trans-opening of the channel, while impermeant PEG4600 was added to the cis side. In both cases impermeant PEG was used to decrease the osmotic pressure gradient across bilayers and, consequently, directional water flux through VDAC-channels that can interfere with PEG partitioning. Open symbols (circles (○) and triangles (△)) represent F^{cis} values obtained at positive and negative voltage, respectively; closed symbols (circles (●) and triangles (▲)) represent F^{trans} values obtained at positive and negative voltage, respectively. More than 160 ion channels were registered under each experimental condition. These two maneuvers gave us two groups of cumulative histograms, which were analyzed the same way as the control one. Mean values of the VDAC-channel conductance in the presence of PEGs on the cis (g^{cis}) or trans (g^{trans}) side of the membrane were corrected for access conductance and then used to calculate F^{cis} and F^{trans} as described in Materials and methods. The error bars are equal or smaller than the symbols used. Vertical arrows indicate the radii values at critical points of VDAC-channel. Division of F^{cis} and F^{trans} dependences into segments was made "by eye". The lowest horizontal segment then was fitted by first-order regression. Other segments were fitted by zero-order regressions. Horizontal arrows indicate filling values at critical points of the trans part of VDAC-channel used to obtain the apparent electrical distance from the openings to the constriction (for details see text). All other experimental conditions are as described in Materials and methods.

technique was discussed previously [15]. It was theoretically ascertained that the access conductance could change the values for the parameter F but should not affect the projection of the turning points of $F-r$ dependence on r-axis, which was used to determine radii of channel lumen. However, this prediction was not tested experimentally. Comparison of this study's results (where the channel conductance was corrected for the access conductance) with the data of Carneiro et al. [11] (obtained with the use of rough values of the VDAC single channel conductance) is the first experimental test of the role of the access conductance in determining the size of ion channel openings by the polymer-exclusion technique. As a result, both studies deduce (from $F-r$ dependencies) practically the same radius for concerned openings of VDAC in high conductance state. Hence, the correction for access conductance does not alter the pore opening size as deduced from the $F-r$ dependence method. However, the correction is important if one would like to study the geometrical features of the lumen because the access conductance correction can change the numerical value of F.

Based on the methods described herein, we argue that the behavior of the $F^{cis}-r$ dependence (after access conductance correction) reflects the cylindrical geometry of the channel lumen seen from the cis opening while the biphasic behavior of the $F^{trans}-r$ dependence suggests a funnel-like geometry at the trans segment of the VDAC channel that may change to a cylindrical geometry further inside the pore.

4.3. The apparent length of the channel parts

As mentioned above, the Porin 31BM channel appears to be a combination of a simple cylinder (the cis part) and a funnel (the trans part). The apparent length of the funnel-like trans part of VDAC channel can be estimated in two steps. First, it has to be determined in terms of the transmembrane potential drop across the channel lumen or in terms of the resistance. As shown elsewhere [6], F is internally related with the transmembrane potential drop at and with resistance of the filled (with a nonelectrolyte) part of the channel lumen. Therefore, F presents the channel length coordinate in relative units, which can be denominated as "electrical distance". In this way the maximal value for F (F_{max}), observed in the presence of the smallest nonelectrolytes, can be assumed to be equal to 1 such unit. The "electrical distance" from the trans opening to the connection between cylindrical and funnel-like structures can be defined as the ratio of filling ($F_i \sim 0.2$) seen for the interception point between the first and the second lines fitted the falling part of $F^{trans}-r$ dependence to the maximal observed filling ($F_{max} \sim 0.7$) (Fig. 2). As a result, the length of the funnel-like trans part of VDAC (in "electrical distance" units, as seen from the trans opening) can be estimated as ~0.3. This means that the trans funnel-like part of VDAC defines ~30% of total channel resistance.

The approximate physical length of these different parts of the channel can be calculated assuming that the conductivity of the solution inside the channel is proportional to the bulk solution conductivity. In this case, the transmembrane potential drops through the channel discontinuously but is piecewise continuous. The total channel resistance (R_{total}) is the sum of two components:

$$R_{cylindrical} + R_{funnel} = \frac{l_{cylindrical}}{\pi r_{cis}^2 k\chi} + \frac{l_{funnel}}{\pi r_{cis} r_{trans} k\chi}$$

where χ is the conductivity of the solution; k is a correction coefficient; r_{cis} and r_{trans} are the maximal radii of the cis and the trans opening estimated from the filling experiments; and $l_{cylinder}$ and l_{funnel} are physical lengths of the cylindrical cis part and the funnel-like trans part of the VDAC channel, respectively. Assuming the total length of the channel ($l_{cylinder}+l_{funnel}$) is equal to 4.6 nm, as determined by 3D

electron microscopy reconstruction of the channel [20], and keeping in mind that $R_{funnel}/(R_{cylindrical}+R_{funnel})=0.3$, the exact values of the length of two parts of the channel can be calculated. The lengths of the cylindrical cis part and the funnel-like trans part of VDAC in high conductance state were estimated to be ~2.5 and ~2.1 nm, respectively.

4.4. Sizes of the openings of the channel in low conductance state

Porin 31BM channels, as the other members of the VDAC family [2,3], are voltage-gated. Specifically, the channel switches to a low conductance state when the applied potential exceeds 30 mV. Several lines of evidence indicate that this transition involves the movement of large portions of the protein [2,19,21]. In agreement with previous results, we observed that when the transmembrane voltage was repeatedly changed from 10 to 50 mV, the single channel currents decreased to different levels, corresponding to a predominant low conductance "state" of the channel. The states with lower conductance did not appear at our experimental conditions.

The low conductance values for each individual channel were calculated and the data obtained on different channels was plotted in cumulative histograms. It appears (Fig. 3) that the low conductance state of Porin 31BM channel was uniform on average. The predominant conductance values for this state were approximately 2.0–3.5 nS. The mean value for this low single channel conductance (2.7 ± 0.4 nS in 1.15 M KCl) was obtained by fitting a single Gaussian line shape to the histogram. This conductance value was found to be approximately half that of high conductance state under identical conditions (4.7 ± 0.4 nS). We then examined the apparent radius of each opening of the channel

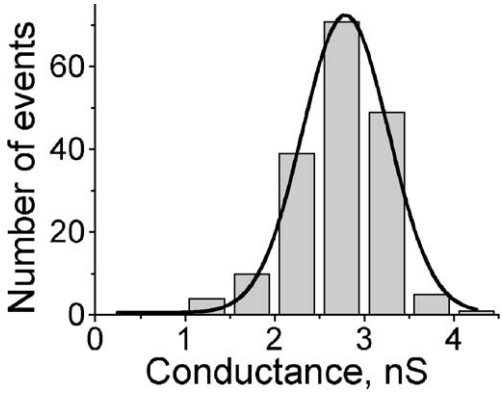

Fig. 3. The amplitude histogram of conductance fluctuations for the low conductance states of the Porin 31 BM channel. The analysis of the channel transitions to the low conductance states was carried out in bilayers containing single VDAC channel. Data presented in the histogram were obtained in more than 30 experiments and constructed from observation of 179 events, with mean values equal to 2.7 ± 0.4 nS. Bin was 0.5 nS. Line (drawn by Microcal Origin, version 5.0 software) indicates theoretical normal distribution of the recorded events. All other conditions are as described in Methods and in the text.

in low conductance state in the presence of differently sized PEGs in the cis (g_c^{cis}) or in the trans (g_c^{trans}) side of the channel. As for the fully open state, small PEGs considerably decreased the conductance of the "closed" states of VDAC (Table 2). Increasing the hydrodynamic radius of PEG caused the VDAC conductance to increase until a new steady-state value was reached at PEG1000 ($r=0.94$ nm) for g_c^{cis} and at PEG2000 ($r=1.22$ nm) for g_c^{trans}. These results suggest that the trans-opening of the VDAC channel is wider than the cis-opening at both the low and high conductance states. However, in the low conductance state, the difference between the two pore opening sizes is much smaller.

The apparent value for the radius of VDAC cis-opening in low conductance state, ~0.9 nm, obtained from $F_c^{cis}-r$ dependence (open squares in Fig. 4), is almost similar to that determined for this opening in the high conductance state (~1.0 nm, Fig. 2). We conclude that the size of the cis opening of the Porin 31BM channel undergoes a weak (if any) alteration during the transition between the two conductance states.

The $F_c^{trans}-r$ relation for the closed state (filled squares in Fig. 4), however, is significantly different from that determined for the channel in the high conductance state (see Fig. 2), especially for polymer molecules with large hydrodynamic radii. When VDAC is in the low conductance state, molecules with r equal to and larger than 1.22 nm (PEG2000) are not able to fill the channel. The relation $F_c^{trans}-r$ is more complex than the $F_c^{cis}-r$, and its decreasing part was fitted with two straight lines. The maximum radius of the trans opening of Porin 31BM channel in low conductance state was estimated to be ~1.2 nm. This value is considerably smaller than that for the channel in the high conductance state (~2.0 nm). Hence, the transition between the high and low conductance states is mainly accompanied by a change in the trans opening. In this state, the channel structure looks more cylindrical than it appears to be in its high conductance state.

To establish the lengths of the cylindrical and funnel-like parts of VDAC channel in the low conductance state, the results were analyzed as the results obtained for the high conductance state. In this way we found that the tentative lengths of the cylindrical and funnel-like parts are ~2.9 and ~1.7 nm, respectively.

Cumulative results demonstrate that the main geometrical change takes place at the trans part of the channel during transition from high to low conductance state.

4.5. VDAC's volume change

Using our data on the geometry of the Porin-31BM-channel and taking the length of the channel as 4.6 nm [20], the volume of the channel lumen can be calculated. We found it to be ~23.3 and ~13.3 nm^3 for high and low conductance states, respectively. Hence, the volume change during channel transition between these two states is around 10 nm^3. This value is smaller and looks more realistic than

Table 2
Conductances of 31BM-porin channel at the low conductance state as changed by PEG addition

		Rough data		Access corrected	
		g_c^{trans} (N)	g_c^{cis} (N)	$g_c\#^{trans}$	$g_c\#^{cis}$
1	Control	2.72 ± 0.41 (169)	2.72 ± 0.41 (169)	3.02	3.02
2	PEG300	1.27 ± 0.26 (117)	1.19 ± 0.21 (141)	1.40	1.31
3	PEG400	1.39 ± 0.10 (108)	1.40 ± 0.13 (217)	1.55	1.57
4	PEG600	1.66 ± 0.26 (56)	1.98 ± 0.43 (231)	1.90	2.33
5	PEG1000	1.93 ± 0.42 (123)	2.38 ± 0.47 (143)	2.26	2.91
6	PEG1450	1.96 ± 0.14 (90)	2.34 ± 0.31 (143)	2.30	2.85
7	PEG2000	2.38 ± 0.18 (45)	2.39 ± 0.33 (97)	2.90	2.92
8	PEG3000	2.33 ± 0.34 (17)	2.33 ± 0.37 (78)	2.83	3.16

Conditions are as described in Methods and in the legend to Table 1.

the volume decrease inferred from analysis of C^{14} glucose flux through VDAC at high and low conductance states (~ 16 nm^3, calculated with assumption of cylindrical geometry of VDAC lumen from data Kulkarni [5]) and from effects of osmotic pressure on mitochondrial VDAC closure (20–40 nm^3 [2]).

From these data the model depicted in Fig. 5 emerges as a geometrical representation of high and low conductance states of the Porin 31BM channel. In high conductance state the radius of the cylindrical part is about 1.0 nm and the length is ~ 2.5 nm. The smaller radius of the conic portion is equal to the radius of the cylindrical part. The larger

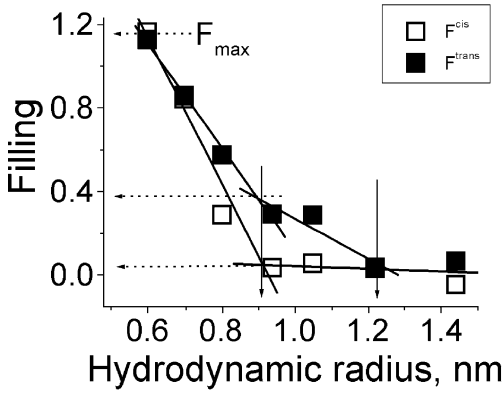

Fig. 4. The dependence of F_c^{cis} (□) and F_c^{trans} (■) (obtained for VDAC-channels in low conductance state) on the hydrodynamic radii of PEGs. More than 30 membranes were used and more than 120 transitions of the ion channels to low conductance state were registered under each experimental condition. The cumulative histograms of low conductance states were built and analyzed as high conductance events. Mean values of the VDAC-channel conductance in the presence of PEGs on the cis (g_c^{cis}) or trans (g_c^{trans}) side of the membrane were corrected for access conductance and then used to calculate F_c^{cis} and F_c^{trans} as described in Materials and methods. The error bars are equal or smaller than the symbols used. Vertical arrows indicate values of the radii of VDAC-channel at critical points. Division of F_c^{cis} and F_c^{trans} dependences into segments was made "by eye". The lowest horizontal segment then was fitted by first-order regression. Other segments were fitted by zero-order regressions. Horizontal arrows indicate filling values at critical points of the trans part of VDAC-channel used to estimate the apparent electrical distances from the openings to the constriction (for details see text). All other experimental conditions are as described in the legend to Fig. 1 and in Materials and methods.

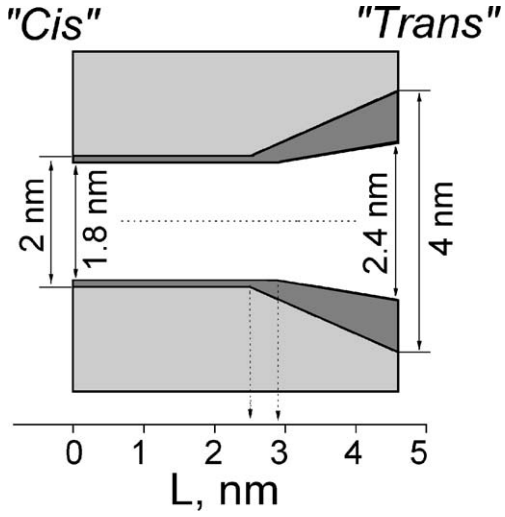

Fig. 5. An inside view on the VDAC channel lumen at high and low conductance states. *L* is the channel length starting from the cis entrance (0 nm) and ending at the trans entrance (4.6 nm). The outer diameter of VDAC channel was taken from the electron microscopy studies [22]. Dashed line represents the central axis of the lumen. Arrows and numbers indicate apparent diameters of the channel openings in high and low conductance states. Dotted lines with arrows indicate the starting point of the funnel part of the channel in high and low conductance states.

radius of the funnel (~ 2.0 nm) is observed at the trans opening of the channel. The length of this portion of the channel is estimated to be 2.1 nm.

It appears that the channel transition to low conductance state is accompanied by a small decrease in the radius (from ~ 1.0 to ~ 0.9 nm) and an increase in the length (from ~ 2.5 to ~ 2.9 nm) of the cylindrical part of the channel at the expense of the trans funnel-like part.

5. Discussion

5.1. Comparison with electron microscopy studies and with β-barrel structure

Considerable information about VDAC's structure has been derived from electron microscopic studies [20,22,23]. Fourier-filtered electron microscopic images suggest that VDAC could be approximated by a nonideal cylinder normal to the membrane plane with a height of ~ 4.6 nm, an outer diameter of about 4.8 nm and an inner diameter of about 2.8 nm. The improved technique allowed revealing the somehow asymmetric pore with several irregular features in the walls [20,22]. Our finding about asymmetry in the geometry of VDAC lumen is generally in accord with these data. In our study VDAC appears to contain two parts: cylindrical (~ 2.5–2.9 nm in length and ~ 2.0 nm in diameter) and funnel-like (1.7–2.1 nm in length and ~ 4 nm in diameter at the pore's opening tapering to ~ 2 nm in diameter further inside the lumen). Comparing our finding with the 3D image obtained from electron microscopic

reconstruction of the channel [20], we can hypothesize that the cylindrical part appears to correlate with the side (~ 3.3 nm in length) of VDAC structure, in which the opening contains only two small indentations.

The other shorter part of the 3D channel image is more indented and has to be compared with the funnel like trans part of the channel seen in nonelectrolyte exclusion method. The topology in that part of the structure does not appear conic at the electron microscopy image. However, it was admitted that this reconstructed topology may represent not the open state but rather the intermediate one (between fully open and particularly closed) [22]. Hence, in the fully open state the topology of that part of the channel may be slightly different from what the electron microscopy shows. So, for example, the dents and/or flaps surrounding this part of the channel could be tilted out for the fully open state of VDAC. Such change in tilt during a channel transition between state is not something unusual: it has been demonstrated with the acetylcholine receptor [24]. Moreover, the presence of the multiple indentations themselves can already participate in the increase in apparent diameter seen by nonelectrolyte exclusion.

As recently shown [25] circular dichroism spectra of fungal VDAC are similar to those of bacterial porins, suggesting that VDAC may be a β-barrel, as are the pores of bacterial outer-membrane channels [26–29]. A more convincing demonstration of structural likeness between bacterial and mitochondrial porins is coming from statistical analysis of protein sequences with a residue motif that corresponds to transmembrane β-strands [30]. A cylindrical co-projection of the 3D shape of VDAC with the Cα backbone of *R. capsulatus* porin [22] demonstrates a good explanation for several indentions and flaps, and additionally indicates the similarity in structures of VDAC and bacterial porins and points out that VDAC may be also constructed with β-strands of different lengths.

Accepting these evidence we could propose that the cylindrical cis part of VDAC could be formed by a β-barrel as it commonly observed for the relatively short (~ 2 nm) β-barrel region of a distinct pore of the trimeric porins [26], or by two sheets of β-strands separated with weaker organized protein domains [22]. The small diameter of this part of VDAC lumen established in this work (~ 1.8–2.0 nm) appears to permit it with less number of β-strands. The number is dependent on the tilt adopted for β-strands. For bacterial porins the tilting angles against the membrane normal vary from about 30° at the membrane facing side at the barrel to about 60° at the interface of three distinct channels. Assuming that the β-strands at the cis part of VDAC have the mean (~ 45°) tilt against the channel axis (what is in accord with Ref. [31]), we can propose that the narrowest cylindrical cis part of VDAC in high (~ 2.0 nm) and low (~ 1.8 nm) conductance states could be constructed from 9–10 or 8–9 β-strands, respectively. The minimal lengths of β-strands, which are sufficient to do this, have to be 3.5–4.1 nm. It is considerably smaller than the length (6.5 nm) needed to construct the barrel (of 4.6 nm height) to penetrate the lipid bilayer. To be in accord with suggested inner geometry of VDAC in high conductance state, one could reasonably assume that the channel is composed of β-strands with unequal lengths (like the bacterial porin does Ref. [26]). The channel looks more uniform on the cis side, where all strands participate in the barrel formation, than on the trans side where the non-complete barrel could be seen. Such "defect" could appear as cavities and/or gloves in the electron microscopy studies and participate in augment of the channel opening shown by nonelectrolyte exclusion technique. This part of the channel may consist in part of β-sheet regions in which strands are tilted more obliquely, and may also contain non-β regions such as loops and/or α-helices. So, we suppose that α-helical N terminus, which localizes on the inner (trans in our study) surface of the outer mitochondrial membrane [32], participates in the formation of the funnel-like trans VDAC opening.

To explain the VDAC transition from high to low conductance state, three main rearrangements in the channel structure have been earlier suggested [22]: the movement of external domain(s) (including the N-terminal α-helix) into the channel lumen surrounded by β-strands, the movement of some domains from the wall of the β-barrel to the surface, and the conformational (β → α transition) changes. Our data suggest that the change in the cylindrical cis β-barrel part of VDAC is small and close to the limit of resolution of the methodology used. Hence, the cylindrical cis part of VDAC could be taken practically unaltered or described in terms of the removal of just one β-strand from the walls of the channel lumen.

The decrease in the apparent size of the trans conic portion of the Porin 31BM channel may be determined by structure rearrangements recently established to occur at different sites of VDAC [21]. Clearly, the molecular rearrangements associated with voltage gating are more complex than the simple movement of contiguous domains of the protein. Different "transmembrane parts" and extramembrane parts of VDAC could be moved at different extents and to different directions to be in accordance with the structural changes observed with electron microscopy [20,33] and in the present study.

5.2. VDAC geometry and conductance

Analyzing the atomic structural models of several ion channels, it was shown [34], that the experimental conductance data should be empirically corrected by a factor of 5 (an average) to predict the effective pore dimension. Theoretical considerations [35] indicate that the calculated conductances will only correlate with experimentally determined ones for very large pores (>10 nm in radius). For narrower channels (as VDAC, for example) the conductance should depend on the molecular nature of the lumen walls. Image force [36] can also take part in the determination of actual channel conductance.

It is widely accepted that hydrophilic as well as hydrophobic molecules are covered by water molecules, forming the so-called hydration water layer. This layer has different properties than the bulk water. It is not active osmotically and is not able to solve ions. The thickness of this layer is around 0.3–0.4 nm. Assuming the presence of this layer of hydration water at the lumen wall (that decreases the effective pore size ion transport), the calculation (made on base of geometrical features established in this study) gives the conductance values for both states of VDAC (5.3 and 3.1 nS) that are very close to the experimental ones preliminarily corrected for access resistors (5.4 and 3.0 nS for high and low conductance state, respectively). The application of the latter approach to other weakly selective channels with known geometry of water lumen (formed by alpha-toxin of *Staphylococcus aureus*, or by cytolysin of *Vibrio cholerae*) gave also an excellent agreement (within 5–10%) between measured and calculated conductances (unpublished data).

Hence, the obtained results demonstrate a good correlation between geometry and conductance for VDAC as well as for other weakly selective channels.

5.3. Method limitations

Measurement of a channel's conductance in the presence of differently sized linear nonelectrolyte polymers—polymer exclusion method—has been used to estimate channel's diameter and to probe asymmetries in its structure [6]. This method is a variation of a technique developed earlier [8] to determine the diameter of larger opening of an ion channel. Although the interpretation of these experiments is based on several simplifying assumptions [14,17,37], the application the HOLE program [34] to directly compare the three-dimensional crystal structure of the cholera toxin B-subunit pentamer channel [38] and the data obtained with polymer exclusion method [39] demonstrates the reliability of the polymer exclusion method.

This approach requires the use of relatively high concentrations of nonelectrolytes (15–20%), which demands special precautions. First of all, polymer-nonelectrolyte behavior at such concentrations (known as the semi-dilute regime) gives relatively poor understanding of polymer physics and one has to utilize mainly empirical approach to analyze the data. The conditions, where there is no nonspecific interaction between nonelectrolyte and the channel wall, have to be chosen. One has to pay attention to possible interference by impurities in the polymer, to effects on ionic activity, to the streaming potentials and to osmotic stress action. Despite these reservations, the approach appears to be very helpful in defining the geometry of the lumen of the channels (and pores) for which there is no structural data. So, a variation of the polymer exclusion method [15] was used to deduce the internal geometry of *S. aureus* α-hemolysin (αHL) ion channel [9] and the channel formed by *V. cholerae* cytolysin [40]. The results are in good agreement with the crystallographic data for α-HL [31] and with electron microscopy data for *V. cholerae* cytolysin [41]. Recently a new very attractive approach for obtaining the internal dimensions of transmembrane pore was suggested [42], combined cysteine mutagenesis and chemical modification. However, it is currently applicable only to pores with known crystallographic structure.

5.4. Concluding remarks

Nonelectrolyte exclusion appears as a reliable method in our study. It allowed us to establish that lumen geometry of VDAC in high conductance state is indeed asymmetric with respect to the center of the membrane. The established asymmetry is virtually independent of the sign of the applied potential. Cumulative data demonstrate that Porin-31BM channels are invariably oriented in planar lipid membranes, and that the internal plasticity of VDAC-channel that can be seen during voltage induced VDAC transition to low conductance state (see, for example, Ref. [21]) does not play a role in determination of the lumen asymmetry at high conductance state.

We also show that the trans side of VDAC channel's lumen undergoes the greatest change in size during the voltage-induced transition to the low conductance state. The apparent change in channel volume during this transition is $\sim 10\ nm^3$.

It appears that taking into account the physical size of the VDAC lumen minus ~ 0.35 nm of hydration water layer at the lumen wall gives a possibility to calculate the channel conductance with a good agreement with measured values.

There is clearly much yet to be learned about the structural states and gating of VDAC. However, we expect that although the suggested model for VDAC may be an oversimplification, it will help to develop a more detailed and less controversial picture of the structure and gating of this interesting and important channel.

Acknowledgements

This work was supported by Conselho Nacional de Desenvolvimento Cientifico e Tecnologico, CNPq, an agency of the Brazilian Government devoted to funding science and technology. We thank Dr. John J. Kasianowicz for helpful comments.

References

[1] J.M. Gulbis, M. Zhou, S. Mann, R. MacKinnon, Structure of the cytoplasmic β subunit-T1 assembly of voltage-dependent K^+ channels, Science 289 (2000) 123–127.
[2] J. Zimmerberg, V.A. Parsegian, Polymer inaccessible volume changes during opening and closing of a voltage-dependent ionic channel, Nature 323 (4) (1986) 36–39.
[3] C. Doring, M. Colombini, Voltage dependence and ion selectivity of the mitochondrial channel, VDAC, are modified by succinic anhydride, J. Membr. Biol. 83 (1–2) (1985) 81–86.

[4] P.N.T. Unwin, P.D. Ennis, Two configurations of a channel-forming membrane protein, Nature 307 (1984) 609–613.
[5] S.V. Kulkarni, Sizing the closed state of the mitochondrial channel, VDAC, Thesis, Department of Zoology, University of Maryland, College Park, Maryland, 1984.
[6] O.V. Krasilnikov, Sizing channel with polymers, in: J.J. Kasianowicz, M.S.Z. Kellermayer, D.W. Deamer (Eds.), Structure and Dynamics of Confined Polymers, Kluwer Publishers, Dordrecht, 2001, pp. 73–91.
[7] L. Jürgens, P. Ilsemann, H.D. Kratzin, D. Hesse, K. Eckart, F.P. Thinnes, N. Hilschmann, Studies of human porin: IV. The primary structures of "Porin 31 HM" purified from human skeletal muscle membranes and of "Porin 31 HL" derived from human B lymphocyte membranes are identical, Biol. Chem. Hoppe-Seyler (Berlin) 372 (1991) 455–463.
[8] R.Z. Sabirov, O.V. Krasilnikov, V.I. Ternovsky, P.G. Merzlyak, Relation between ionic channel conductance and conductivity of media containing different non-electrolytes. A novel method of pore size determination, Gen. Physiol. Biophys. 12 (1993) 95–111.
[9] P.G. Merzlyak, L.N. Yuldasheva, C.G. Rodrigues, C.M.M. Carneiro, O.V. Krasilnikov, S.M. Bezrukov, Polymeric nonelectrolytes to probe pore geometry: application to the alpha-Toxin transmembrane channel, Biophys. J. 77 (1999) 3023–3033.
[10] P. Mueller, D.O. Rudin, H.T. Tien, W.C. Wescott, Methods for the formation of single bimolecular lipid membranes in aqueous solution, J. Phys. Chem. 67 (1963) 534–535.
[11] C.M.M. Carneiro, O.V. Krasilnikov, L.N. Yuldasheva, A.C. Campos de Carvalho, R.A. Nogueira, Is the mammalian porin channel, VDAC, a perfect cylinder in high conductance state? FEBS Lett. 416 (1997) 187–189.
[12] R. Pfaller, R. Kleene, W. Neupert, Biogenesis of mitochondrial porin: the import pathway, Experientia 46 (2) (1990) 153–161.
[13] R. Benz, E. Maier, F.P. Thinnes, H. Gotz, N. Hilschmann, Studies on Human Porin: VII. The channel properties of the human B-lymphocyte membrane-derived "Porin 31HL" are similar to those of mitochondrial porins, Biol. Chem. Hoppe-Seyler 373 (1992) 295–303.
[14] S.M. Bezrukov, I. Vodyanoy, Probing alamethicin channels with water-soluble polymers: effect on conductance of channel states, Biophys. J. 64 (1993) 16–25.
[15] O.V. Krasilnikov, J.B. Da Cruz, L.N. Yuldasheva, R.A. Nogueira, A novel approach to study the geometry of the water lumen ion channel. Colicin Ia channels in lipid bilayers, J. Membr. Biol. 161 (1) (1998) 83–92.
[16] J.E. Hall, Access resistance of a small circular pore, J. Gen. Physiol. 66 (1975) 531–532.
[17] S.M. Bezrukov, I. Vodyanoy, R.A. Brutyan, J.J. Kasianowicz, Dynamics and free energy of polymers partitioning into a nanoscale pore, Macromolecules 29 (1996) 8517–8522.
[18] S.M. Bezrukov, J.J. Kasianowicz, The charge state of an ion channel controls neutral polymer entry into its pore, Eur. Biophys. J. 26 (1997) 471–476.
[19] L. Thomas, E. Blachly-Dyson, M. Colombini, M. Forte, Mapping of residues forming the voltage sensor of the voltage-dependent anion-selective channel, Proc. Natl. Acad. Sci. U. S. A. 90 (1993) 5446–5449.
[20] X.W. Guo, P.R. Smith, B. Cognon, D. D'Arcangelis, E. Dolginova, C.A. Mannella, Molecular design of the voltage-dependent, anion-selective channel in the mitochondrial outer membrane, J. Struct. Biol. 114 (1995) 41–59.
[21] J. Song, C. Midson, E. Blachly-Dison, M. Forte, M. Colombini, The sensor region of VDAC is translocated from within the membrane to the surface during the gating processes, Biophys. J. 74 (1998) 2926–2944.
[22] C.A. Mannella, Conformational changes in the mitochondrial channel protein, VDAC, and their functional implications, J. Struct. Biol. 121 (1998) 207–218.
[23] X.W. Guo, C.A. Mannella, Conformational change in the mitochondrial channel, VDAC, detected by electron cryo-microscopy, Biophys. J. 64 (1993) 545–549.
[24] N. Unwin, A. Miyazawa, J. Li, Y. Fujiyoshi, Activation of the nicotinic acetylcholine receptor involves a switch in conformation of the alpha subunits, J. Mol. Biol. 319 (5) (2002) 1165–1176.
[25] L. Shao, K.W. Kinnally, C.A. Mannella, Circular dichroism studies of the mitochondrial channel, VDAC, from *Neurospora crassa*, Biophys. J. 71 (2) (1996) 778–786.
[26] M.S. Weiss, A. Kreusch, E. Schiltz, U. Nestel, W. Ewelte, J. Weckesser, G.E. Schulz, The structure of porin from *Rodobacter capsulatus* at 1.8 A resolution, FEBS Lett. 280 (2) (1991) 379–382.
[27] M.S. Weiss, G.E. Schulz, Structure of porin refined at 1.8 A resolution, J. Mol. Biol. 227 (1992) 493–509.
[28] S.W. Cowan, T. Schirner, G. Rummel, M. Steiert, R. Ghosh, R.A. Pauptit, J.N. Jansonius, J.P. Rosenbusch, Crystal structures explain functional properties of two *E. coli* porins, Nature 358 (1992) 727–733.
[29] T. Schirmer, T.A. Keller, Y.F. Wang, J.P. Rosenbusch, Structural basis for sugar translocation through maltoporin channels at 3.1 A resolution, Science 267 (1995) 512–514.
[30] C.A. Mannella, A.F. Neuwald, C.E. Lawrence, Detection of likely transmembrane β-strand regions in sequences of mitochondrial pore proteins using the Gibbs Sampler, J. Bioenerg. Biomembr. 18 (2) (1996) 163–169.
[31] L. Song, M.R. Hobaugh, C. Shustak, S. Cheley, H. Bayley, J.E. Gouaux, Structure of staphylococcal α-hemolysin, a heptameric transmembrane pore, Science 274 (1996) 1859–1866.
[32] S.A. Konstantinova, C.A. Mannella, V.P. Skulachev, D.B. Zorov, Immunoelectron microscopic study of the distribution of porin on outer membranes of rat heart mitochondria, J. Bioenerg. Biomembr. 27 (1995) 93–99.
[33] C.A. Mannella, Structural analysis of mitochondrial pores, Experiencia 46 (1990) 137–145.
[34] O.S. Smart, J. Breed, G.R. Smith, M.S.P. Samsom, A novel method for structure-based prediction of ion channel conductance properties, Biophys. J. 72 (1997) 1109–1126.
[35] C.A. Pasternak, C.L. Bashford, Y.E. Korchev, T.K. Rostovtseva, A.A. Lev, Modulation of surface flow by divalent cations and protons, Colloids Surf. 77 (1993) 119–124.
[36] S.C. Li, M. Hoyles, S. Kuyucak, S.H. Chung, Brownian dynamics study of ion transport in the vestibule of membrane channels, Biophys. J. 74 (1) (1998) 37–47.
[37] V.I. Ternovsky, G.N. Berestovsky, Effective diameter and structural organization of reconstituted calcium channels from the Characeae algae *Nitellopsis*, Membr. Cell Biol. 12 (1) (1998) 79–88.
[38] R.G. Zhang, D.L. Scott, M.L. Westbrook, S. Nance, B.D. Spangler, G.G. Shipley, E.M. Westbrook, The three dimensional crystal structure of cholera toxin, J. Mol. Biol. 251 (1995) 563–573.
[39] O.V. Krasilnikov, J.N. Muratkhodjaev, S.E. Voronov, Y.V. Yezepchuk, The ionic channels formed by cholera toxin in planar bilayer lipid membranes are entirely attributable to its B-subunit, Biochim. Biophys. Acta 1067 (1991) 166–170.
[40] L.N. Yuldasheva, P.G. Merzlyak, A.O. Zitzer, C.G. Rodrigues, S. Bhakdi, O.V. Krasilnikov, Lumen geometry of ion channels formed by *Vibrio cholerae* EL Tor cytolysin elucidated by nonelectrolyte exclusion, Biochim. Biophys. Acta 1512 (2001) 53–63.
[41] A. Zitzer, M. Palmer, U. Weller, T. Wassenaar, C. Biermann, J. Tranum-Jensen, S. Bhakdi, Mode of primary binding to target membranes and pore formation induced by *Vibrio cholerae* cytolysin (hemolysin), Eur. J. Biochem. 247 (1997) 209–216.
[42] L. Movileanu, S. Cheley, S. Howorka, O. Braha, H. Bayley, Location of a constriction in the lumen of a transmembrane pore by target covalent attachment of polymer molecules, J. Gen. Physiol. 117 (2001) 239–251.